7-2020

Probing Cooperativity In C–H···N and C–H···π Interactions: Dissociation Energies Of Aniline···$(CH_4)_n$ (n = 1, 2) van der Waals Complexes From Resonant Ionization And Velocity Mapped Ion Imaging Measurements

James Makuvaza
Marquette University

John L. Loman
Marquette University

Damian L. Kokkin
Marquette University

Scott Reid
Marquette University, scott.reid@marquette.edu

The Journal of Chemical Physics ARTICLE scitation.org/journal/jcp

Probing cooperativity in C–H···N and C–H···π interactions: Dissociation energies of aniline···$(CH_4)_n$ (n = 1, 2) van der Waals complexes from resonant ionization and velocity mapped ion imaging measurements

Cite as: J. Chem. Phys. 153, 044303 (2020); doi: 10.1063/5.0015624
Submitted: 29 May 2020 • Accepted: 7 July 2020 •
Published Online: 27 July 2020

James T. Makuvaza, John L. Loman, Damian L. Kokkin, and Scott A. Reid[a)]

AFFILIATIONS

Department of Chemistry, Marquette University, Milwaukee, Wisconsin 53233, USA

[a)]**Author to whom correspondence should be addressed:** scott.reid@marquette.edu. **Telephone:** (414) 288-7565

ABSTRACT

Recent studies of the weakly bound anisole···CH_4 complex found a dual mode of binding, featuring both C/H···π and C/H···O noncovalent interactions. In this work, we examine the dissociation energies of related aniline···$(CH_4)_n$ (n = 1, 2) van der Waals clusters, where both C/H···π and C/H···N interactions are possible. Using a combination of theory and experiments that include mass-selected two-color resonant two-photon ionization spectroscopy, two-color appearance potential (2CAP) measurements, and velocity-mapped ion imaging (VMI), we derive the dissociation energies of both complexes in the ground (S_0), excited (S_1), and cation radical (D_0) states. As the amide group is non-planar in the ground state, the optimized ground state geometry of the aniline···CH_4 1:1 complex shows two isomers, each with the methane positioned above the aniline ring. The observed redshift of the electronic origin from the aniline monomer is consistent with TDDFT calculations for the more stable isomer, where the methane sits on the same face as the amino hydrogens. The dissociation energies of the 1:1 complex, obtained from 2CAP measurements, are in good agreement with the calculated theoretical values from selected density functional theory methods. VMI data for the 1:1 complex gave a binding energy value overestimated by ~179 cm^{-1} when compared to the 2CAP results, indicating that dissociative ionization selectively populates an excited vibrational level of the aniline cation radical. Given that the electron donating ability of aromatic substituents trends as $-NH_2 > -OCH_3 > -CH_3$, it is noteworthy that the strength of methane binding also trends in this order, as found by experiment (dissociation energies in kJ/mol: 6.6 > 5.8 > 4.5) and predicted by theory (PBE0-D3/def2-QZVPPD, in kJ/mol: 6.9 > 6.0 > 5.0). For the 1:2 complex of aniline and methane, calculations predict that the more stable conformer is the one where the two methane molecules lie on opposite faces of the ring, consistent with the observed redshift of the electronic origin. Unlike the anisole–methane 1:2 complex, which shows an enhanced dissociation energy for the loss of one methane in comparison with the 1:1 complex, here, we find that the energy required to remove one methane from the ground state aniline–methane 1:2 complex is smaller than that of the 1:1 complex, consistent with theoretical expectations.

INTRODUCTION

The study of molecular complexes provides a platform for understanding non-covalent interactions, which are important in many areas of science. Such interactions include hydrogen bonding,[1–3] π–π stacking,[4–8] C/H–π,[4,7,9–12] C/H–O,[9,13,14] and halogen bonding, and other σ-hole types of interactions.[15,16] These play a pivotal role in the structure of proteins and biomolecules,[13]

drug–substrate interactions,[17,18] anion recognition,[15,19] crystal engineering,[6] molecular self-assembly, and supramolecular chemistry.[14,20,21] Insight into all of these processes is gleaned from the study of small complexes, which provides a bridge from isolated gas-phase molecules to condensed phases, enabling us to gain invaluable insights into solvation processes, solution dynamics, and the nucleation and growth of complexes.[22–26] By exploiting a solute chromophore (typically an aromatic), complexes with various solvents (e.g., rare gas atoms or small molecules) have been studied in the gas-phase using a variety of spectroscopic techniques, supplemented by theoretical methods, to determine the spectroscopic features, geometry, and binding interactions.[22–32]

Aniline is the simplest aromatic amine and is amenable to ionization and detection via mass selective resonant two-photon ionization (R2PI) methods.[33–35] The spectroscopy of aniline in the S_0, S_1, and D_0 states has been studied in detail.[33–36] It has been firmly established that the molecule is nonplanar in the S_0 state but becomes essentially planar in the S_1 and D_0 states due to a significant lowering of the barrier to inversion of the amino hydrogens upon electronic excitation and ionization, respectively. A variety of studies have been reported on the formation and characterization of van der Waals complexes of aniline with rare gases,[37–51] small molecules,[52–59] and larger molecules/aromatics.[60–65] Furthermore, the homocomplexes of aniline have been studied by both infrared (IR) and R2PI spectroscopies.[66–70]

In a recent paper, we examined the 1:1 complex of anisole with methane,[9] where a dual modality of binding was exhibited, with the methane interacting with both the oxygen and conjugated π systems through C/H···O and C/H···π interactions. Like anisole, aniline possesses two sites that can act as proton acceptors, the electron lone pair on nitrogen and the conjugated π system, and thus, both C/H···π and C/H···N types of interactions can be expected for the aniline···CH_4 complex. In addition, the amino hydrogens of aniline can also afford hydrogen bonding with solvents containing O or N atoms. Unlike anisole, the planarization of the amino group, which occurs upon electronic excitation or ionization of aniline, may significantly impact the structure and energetics of binding in these states. We note that C/H···N interactions have emerged as important binding motifs in molecular self-assembly, protein structure, and crystal engineering.[13,71–76]

Prior studies have examined the spectroscopy of the aniline···$(CH_4)n$ (n = 1, 2) complexes; however, the dissociation energies have not been accurately determined. In 1984, Bernstein *et al.* examined the spectroscopy of the 1:1 complex and estimated an upper limit to the dissociation energy in the S_1 state of ~699 cm^{-1} (8.4 kJ/mol) from the onset of monomer fluorescence.[56] In 1989, the same group revised this estimate downward to 480 cm^{-1} (5.7 kJ/mol) by observing the absence of higher vibronic bands from a two-color excitation spectrum and using a Rice–Ramsperger–Kassel–Marcus (RRKM) model analysis to fit the observed vibrational predissociation rates.[57] Subsequently, Zhang *et al.* used photoelectron spectroscopy to predict the change in dissociation energy of the aniline···CH_4 complex upon ionization from ionization potential (IP) measurements of the monomer and the complex.[58] For the D_0 state, the dissociation energy was predicted to increase by 169 cm^{-1} and 92 cm^{-1}, respectively, compared to that in the S_0 and S_1 states. A later study by the Knee group, which employed picosecond photoelectron spectroscopy, reported a S_1 state dissociation energy of 450 cm^{-1} (5.4 kJ/mol) from an RRKM model analysis.[59] Thus, some ambiguity remains concerning the dissociation energies of the 1:1 complex of aniline and methane, and a direct experimental measurement is desired.

Building upon our prior studies of related anisole–methane complexes,[9] the goal of this work is to accurately determine the dissociation energies of the aniline···$(CH_4)_n$ (n = 1, 2) complexes in the three respective states (S_0, S_1, and D_0). Thus, here, we report on the measurement of the dissociation energies of the aniline···$(CH_4)_n$ (n = 1, 2) complexes using a combination of experimental methods, including two-color R2PI or 2CR2PI, two-color appearance potential measurements or 2CAP, and velocity-mapped ion imaging or VMI. Our experimental findings are compared with the results of selected theoretical (density functional theory or DFT) methods. In addition to being used as a benchmark for theoretical studies, experimental dissociation energy measurements can also afford important insights into competitive non-covalent interactions and cooperativity, i.e., how the binding of the first "solvent" molecule affects the binding of the second. In studies of anisole–methane complexes, we found that the dissociation energy of methane loss from the 1:2 complex increased by 10% with respect to that of the 1:1 complex, although both solvent molecules occupied similar sites on opposite faces of the aromatic ring. The related model systems such as the benzene and toluene···CH_4 complexes have also been used to investigate such effects.[77–82]

EXPERIMENTAL AND THEORETICAL METHODS

The experimental approach employed in this work is very similar to that described in a recent publication.[9] Briefly, it consisted of a TOF mass spectrometer equipped with a pulsed nozzle. Two frequency-doubled Nd/YAG pumped dye lasers were used for excitation/ionization, and an 8-channel digital pulse delay generator was used for temporal control of the experiment. Aniline (99.5%, Sigma-Aldrich) soaked cotton swabs were placed in a temperature-controlled oven that was connected to the inlet of a pulsed nozzle. The oven and nozzle were heated to 60 °C. At this temperature, the aniline vapor pressure is roughly 6.5 Torr, as estimated from the Antoine equation parameters.[83] A mixture of 5% methane in Ar carrier gas at a backing pressure of 50 psi was passed through the heated oven, picking up the aniline vapor, and then injected into the TOF source chamber through the 0.8 mm diameter orifice of the pulsed nozzle, forming a molecular beam. The beam passed through a 1.5 mm diameter conical nickel skimmer before entering the ionization region of the TOF. Resonant excitation and ionization were achieved using the outputs of two independently tunable frequency-doubled Nd/YAG pumped dye lasers, Sirah Cobra-Stretch and Lambda-Physik Scanmate 2E, pumped by the second harmonic of a Spectra-Physics INDI and Quantel Q-Smart 850, respectively. As the aniline S_1 lifetime is relatively short, or order 2 ns–3 ns,[84,85] for all of the experiments reported here, the laser pulses were overlapped temporally. Typical laser fluences were of order 0.1 mJ, with the beams loosely focused into the ionization region using 2 m spherical lenses. The ions were extracted via a three-plate stack and flew a distance of 1 m before striking a dual chevron microchannel plate detector.

Ion yield spectra for the aniline monomer, and aniline···CH_4 1:1 and 1:2 complexes, were determined by setting the pump laser (λ_1) on resonance and scanning the frequency of the second laser (λ_2) through the ionization threshold, monitoring the onset of the monomer or complex ion signal. To determine the S_0 state binding energy of the 1:1 and 1:2 complexes, 2CAP measurements were performed, where the pump laser was set on resonance (λ_1) of the complex of interest, and the second (ionizing) laser (λ_2) was scanned above the dissociation threshold while monitoring the mass channel of the fragment species of interest.

Velocity-mapped ion imaging experiments were carried out in a separate spectrometer that utilized the same beam conditions and laser configuration, which are described in detail in our previous publication.[9] The counter propagating lasers intercepted the molecular beam between the repeller and extractor electrodes, downstream of the skimmer orifice. The voltages of the electrodes were tuned precisely for optimum velocity mapping conditions. During image acquisition, the rear MCP voltage was gated to monitor the species of interest. Images were collected above and below the dissociation threshold, over a period of 60 min. Typically, 36 000 laser shots were acquired, with the signal attenuated using a linear polarizer to avoid image blurring by ensuring that only a few ions were detected each shot. Images collected at energies above the dissociation threshold were background-corrected using images obtained with the second photon set below the dissociation threshold. The resultant images were inverse Abel transformed using a pBASEX algorithm in a LABVIEW coded program.

The experimental protocol was as follows: Initially, the electronic spectra of the aniline···$(CH_4)_n$ (n = 1, 2) complexes were obtained using R2PI spectroscopy. Subsequently, 2CR2PI measurements with a tunable ionizing photon were performed to derive the ion yield spectra of the aniline monomer and the 1:1 and 1:2 complexes of aniline and methane from which the respective ionization potentials (IPs) were derived. Then, 2CAP measurements were conducted on the jet cooled aniline···CH_4 and aniline···$(CH_4)_2$ complexes to determine binding energies in their ground states (S_0). A thermochemical cycle analysis then returned upper limits of binding energies in the first excited state (S_1) and cation radical state (D_0). We then carried out VMI measurements to directly measure the binding energy in the D_0 state, and application of the thermochemical cycle afforded the corresponding binding energies for the S_1 and S_0 states.

Electronic structure calculations were performed to estimate the equilibrium geometries and energetics of aniline and the aniline–methane 1:1 and 1:2 complexes using the Gaussian 09 software package. Our previous study of dispersion dominated, fluorene based π-stacked dimers revealed that PBE0 and M06-2X density functionals augmented with Grimme's D3 dispersion term[86] well reproduced the ground state binding energy but overestimated the binding in the excited and cation radical states.[8] In contrast, the CAM-B3LYP-D3 functional with def2-QZVPPD or 6-311++G(3df, 3pd) basis sets reproduced in the most balanced way the dissociation energies across all three states. Recently, dissociation energies calculated using various DFT and *ab initio* methods were benchmarked against experimental values for the anisole···CH_4 complex in the S_0 and D_0 states, and it was found that the PBE0, CAM-B3LYP, and M06–2X methods with a 6-311++G(3pd,3df) basis set well reproduced the experimental results across the two states (S_0, D_0).[9] Accordingly, here, we performed complete geometry optimizations on the aniline···CH_4 complex. After optimization, vibrational frequency calculations were performed to confirm that the optimized structure(s) corresponded to minima on the potential energy surface. The derived dissociation (binding) energies were corrected for zero-point vibrational energy (ZPVE). For the basis set used here (def2-QZVPPD), the basis set superposition error (BSSE) corrections were negligible (i.e., <0.2 kJ/mol). The calculated dissociation energies were compared with experimental data from 2CAP and VMI measurements.

RESULTS AND DISCUSSION

Aniline···CH_4 1:1 complex

Figure 1 shows an overview of the spectroscopic information collected for the aniline monomer and 1:1 aniline···CH_4 complex, presented with an energy ladder diagram in the S_0, S_1, and D_0 states, respectively. Data for the aniline monomer were obtained using expansions of aniline in Ar. The electronic spectra, obtained via 2CR2PI spectroscopy, are presented in the lower panels of Fig. 1. The electronic origin of the complex is red shifted by −81 cm^{-1} with respect to the monomer origin, consistent with previous publications.[56–59] Often, van der Waals complexes involving a π system are more strongly bound in the excited state and exhibit a red shift due to the delocalization of the electronic cloud. Noticeably, the shift here is significantly larger than observed for 1:1 complexes of CH_4 with benzene (−41 cm^{-1}), toluene (−43 cm^{-1}), and anisole (−64 cm^{-1}).[9,77,78]

Following the measurement of the excitation spectra using a 2CR2PI scheme with a fixed ionizing photon wavelength, we then set the excitation wavelength to the respective electronic origins and measured the ion yield spectra of aniline and the aniline···CH_4 complex to determine the respective ionization potentials (shown in the upper panels in Fig. 1). The relatively well defined onsets are observed from the spectra of the monomer and complex, which gave the following IP values: aniline, 7.723 eV and aniline···CH_4 complex,

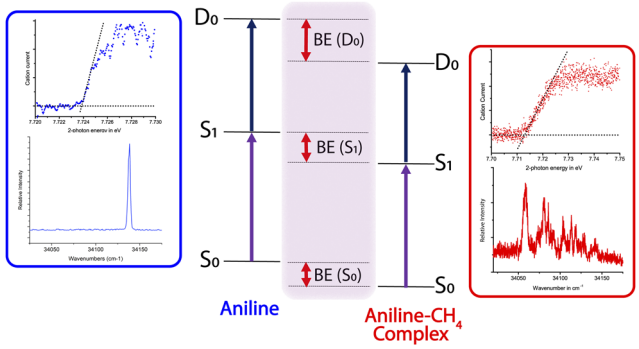

FIG. 1. Spectroscopic data for aniline and the 1:1 aniline···methane complex. The lower figure in each panel shows the electronic spectrum, obtained via 2CR2PI spectroscopy, while the upper figure in each panel displays the ion yield curve from which the ionization potential was determined. The ladder diagram links the energy levels of the monomer and complex.

7.711 eV, with our measured IP values slightly higher than previous determinations, monomer (7.7206 eV) and complex (7.701 eV).[58,87] We note that our IP values are not corrected for shifts due to the electric fields inevitably present in the ionization region, as the primary focus of our measurement is the determination of dissociation energies taken from the *difference* in IPs of the monomer and complex.

To assign the isomeric structure of the complex, we carried out theoretical calculations. Initial geometry optimizations were performed at the PBE0/def2-TZVPPD level and subsequently refined at the PBE0/def2-QZVPPD level. These calculations identified two isomeric structures—in each the methane sits above the aromatic plane (Fig. 2) and interacts with aniline via C–H/N and C–H/π interactions, a dual-mode of interaction similar to that observed in the anisole–methane complex.[9] Interestingly, these calculations predict that isomer 2, where the methane sits on the same face as the amino hydrogens, is the more stable. The coordinates for the optimized structures are provided in the supplementary material.

To identify which isomer(s) might be contributing to the observed 2CR2PI spectrum, we performed calculations using time-dependent DFT (TDDFT), at the TDPBE0-D3/def2-QZVPPD level, on the PBE0-D3/def2-QZVPPD optimized structures. As shown in Table S1 of the supplementary material, these calculations predict redshifts of 35 cm^{-1} and 85 cm^{-1} for isomers 1 and 2, respectively. Thus, while both isomers may contribute to the observed spectrum, it appears that the most redshifted band is consistent with the origin of isomeric complex 2, the most stable complex as predicted both by the calculations presented above and additional calculations that we outline below. In this work, we used this feature to derive the ion yield spectra (Fig. 1) and both 2CAP spectra and VMI results presented below. Thus, for the remainder of this paper, we will assume that the structure of the 1:1 complex conforms to isomer 2.

In order to estimate the ground (S_0) state binding energy of the 1:1 complex, we performed two-color appearance potential (2CAP) measurements, which set an upper limit to the binding energy. Here, the excitation laser was fixed on the origin of the complex, and the ionization laser was scanned while monitoring the signal in the mass channel of the aniline cation. The energetic onset of the aniline cation can be represented as the sum of the ground (S_0) state complex binding energy and the adiabatic complex ionization energy, as illustrated in Fig. 3(a). The 2CAP spectrum of the aniline···CH_4 1:1 complex is shown in Fig. 3(b), where the energy scale was determined by subtracting the monomer IP from the two-photon excitation energy, and thus, it provides a direct readout of the ground state dissociation energy. A clear onset representing the appearance potential was observed, and a linear extrapolation of the rising edge returns an upper limit to the S_0 state dissociation energy of 6.6(2) kJ/mol or ~550 cm^{-1}, in excellent agreement with the PBE0/def2-QZVPPD prediction for isomer 2.

Application of the thermochemical cycle shown in Fig. 1 affords the dissociation energy in the excited (S_1) and cation radical (D_0) states, presented in Table I in units of kJ/mol. The value derived for the S_1 state binding energy is 7.6 kJ/mol or 640 cm^{-1}. It is noteworthy that the 2CAP data show an increase in binding energies between S_0 and S_1, but a similar binding energy for S_1 and D_0.

In addition to the 2CAP measurements, VMI experiments were also performed. Complementary to the 2CAP results, the VMI measurements provide a direct measure of the kinetic energy (KE) release to the monomeric cation following ionization-induced fragmentation. Thus, this method can provide a direct estimate of the dissociation energy in the *cation radical state* (D_0). Shown in Fig. 4 (left panel) are VMI images of the aniline cation obtained at the total (two-photon) energies shown, which span one energy below and three above the dissociation threshold of the aniline···CH_4 complex. Images taken at total energies above the dissociation threshold were background subtracted and inverse Abel transformed, and the kinetic energy (KE) distributions obtained following transformation are shown in the right panel of Fig. 4.

From the data shown in Fig. 4, it is apparent that KE_{max}, which reflects the complex dissociation energy assuming the formation of cold (ground state) monomer cation, scales in proportion

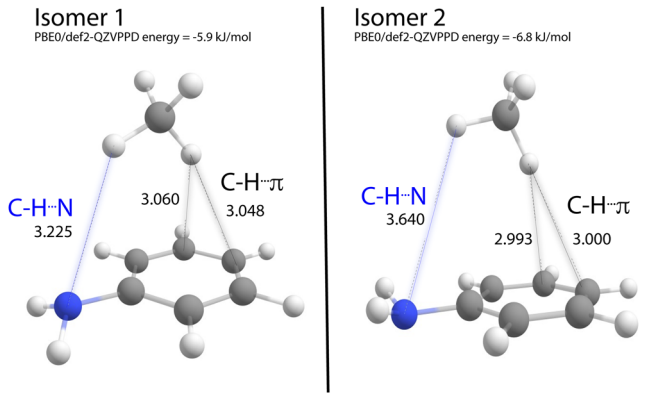

FIG. 2. Isomeric structures of the aniline–methane 1:1 complex calculated at the PBE0/def2-QZVPPD level. The energies reflect the stabilization of the complex with respect to the isolated monomers and are corrected for ZPE. With this basis set, the BSSE correction is negligible.

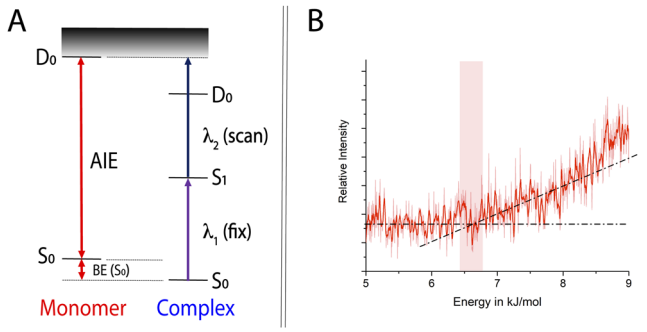

FIG. 3. (a) Illustration of the 2CAP method. Appearance energy of the monomer fragment is represented as the sum of ground state binding energy of the complex and adiabatic ionization energy (AIE) of the monomer. (b) 2CAP spectrum of the aniline–methane complex, where the energy axis is scaled to show the ground state dissociation energy in kJ/mol. The darker line in this panel represents a 10 point smoothing of the data.

TABLE I. Comparison of experimental and computed dissociation energies for the aniline–methane 1:1 complex. All theoretical energies were corrected for ZPE, while the BSSE correction was negligible with the employed basis set. Unrestricted wavefunctions were employed for calculations of the cation radical state.

	Dissociation energy (kJ/mol)		
Method	S_0	S_1	D_0
Experiment (this work, 2CAP)	6.6(3)	7.6(3)	7.8(3)
Experiment (this work, VMI, uncorrected)	8.7(2)	9.7(2)	9.9(2)
Experiment (this work, VMI, corrected)	6.6(2)	7.6(2)	7.8(2)
Experiment (Ref. 56)		8.4	
Experiment (Ref. 57)		5.7	
Experiment (Ref. 58)			S_1 DE + 1.1 S_0 DE + 1.9
Experiment (Ref. 59)		5.4	
CAM-B3LYP-D3/def2-QZVPPD	6.0	...	7.6
M062X-D3/def2-QZVPPD	6.2	...	7.8
PBE0-D3/def2-QZVPPD	6.9	...	8.3

to the total energy, as expected. A dissociation energy in the D_0 state (9.9 kJ/mol or 830 cm^{-1}) was determined from the observed KE_{max}, derived from an extrapolation of the data to the baseline, and the total available energy and is an average of measurements taken at three different total energies. Using the energetic cycle derived from spectroscopic data (Fig. 1), the dissociation energies in S_0 and S_1 were then determined, and these are provided in Table I.

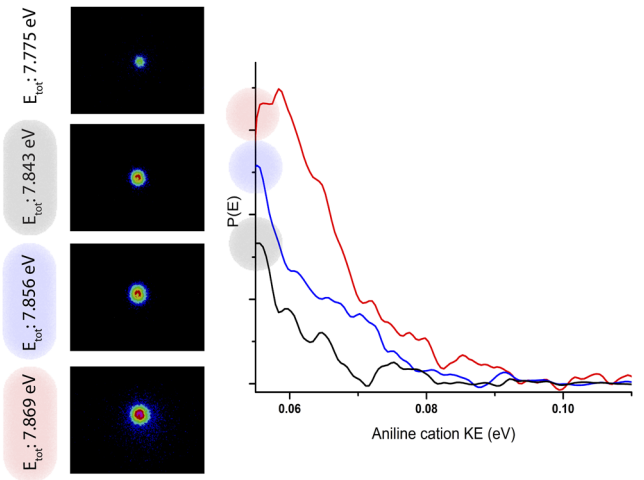

FIG. 4. Left: aniline monomer ion images obtained following the dissociation of the aniline···CH_4 complex at four different total energies indicated, corresponding to one energy below (top) and three above the complex dissociation threshold. Right: the P(E) distributions obtained following the transformation of the three images collected above the dissociation threshold. The maximum kinetic energy values from the plots were used to determine the D_0 state binding energy, as described in the text.

Unlike our prior study of anisole–methane complexes,[9] here, the 2CAP and VMI experiments do not agree regarding the aniline–CH_4 dissociation energy in the D_0 state (Table I). As the VMI experiments are analyzed with the assumption that KE_{max} corresponds to the formation of vibrationally cold fragments, one possible explanation for this discrepancy is the preferential formation of the vibrationally excited aniline cation radical in the VMI experiments. Indeed, this was previously observed in VMI measurements of the anisole dimer.[88] The difference in D_0 state binding energy between the VMI and 2CAP results is ~180 cm^{-1}, which corresponds exactly to the lowest vibrational frequency (10b) of the aniline cation, an out-of-plane NH_2 wag ring deformation. Thus, the discrepancy between the 2CAP and VMI measurements can be resolved if it is assumed that the aniline cation fragment is preferentially produced with one quantum of excitation in mode 10b following dissociation of the ionized aniline···CH_4 complex. With this assumption, the corrected dissociation energy values are reported in Table I, in good agreement with the 2CAP measurement. This illustrates the benefit of comparing VMI measurements with those from 2CAP (or other methods) to identify cases where dissociation preferentially populates excited vibrational states.[42]

Regarding comparison with previous experiments, these are also listed in Table I. Our S_1 dissociation energy lies between the two experimental values derived by Bernstein[56,57] and is roughly 2 kJ/mol higher than that estimated by Smith *et al.*[59] The *difference* in S_0 and S_1 dissociation energies that we measure is in good agreement with that derived in Ref. 58.

To aid in understanding the experimental results, we performed additional calculations of the complex geometry, spectroscopic properties, and dissociation energies of isomer 2 using theoretical methods, including dispersion corrected single and double hybrid density functional theory methods (PBE0-D3, M062X-D3, and Cam-B3LYP-D3) with def2-XZVPPD (X = T, Q). The calculated dissociation energies were corrected for zero-point energy (ZPE)—in practice, we found that the BSSE correction was negligible (i.e., <0.2 kJ/mol) when employing the larger basis set (def2-QZVPPD).

The calculated ground state dissociation energies (Table I) range from 6.0 kJ/mol to 6.9 kJ/mol, in close agreement with the 2CAP and corrected VMI estimates. For all of the theoretical methods, the predicted difference in energy of the two isomers was similar, of order ~1 kJ/mol, with isomer 2 as the global minimum energy structure.

Considering the D_0 state, complete geometry optimizations were performed using spin unrestricted wavefunctions at the various levels of theory presented in Table I. The estimated dissociation energies were also corrected for ZPE, again the BSSE correction became insignificant with this basis set. The optimized structure of the complex cation radical at the UPBE0-D3/def2-QZVPPD level of theory is shown in Fig. S1 of the supplementary material. The calculated D_0 dissociation energies range from 7.6 kJ/mol to 8.3 kJ/mol, in excellent agreement with the experimental 2CAP and corrected VMI results.

The experimental and theoretical predictions of the 1:1 complex structure are suggestive of a dual mode of non-covalent interaction (Fig. 1). The measured S_0 state dissociation energy is approximately additive if we consider the previously determined interaction energies for complexes exhibiting only C/H···π interactions such as benzene or toluene···CH_4 (~4.315 kJ/mol–4.5 kJ/mol)[77–79] and C/H···N interactions in the prototypical ammonia···CH_4 complex (~2.5 kJ/mol). The experimental result suggests that the bond dissociation energy of a C/H···N type of interaction (~2.5 kJ/mol) is stronger than that of the previously determined C/H···O interaction (~1 kJ/mol).[9] Considering that the electron donating ability of aromatic substituents trends as $-NH_2 > -OCH_3 > -CH_3$, it is noteworthy that the strength of methane binding also trends in this order for aniline, anisole, and toluene, as found by experiment (dissociation energies in kJ/mol: 6.6 > 5.8 > 4.5) and predicted by theory (PBE0-D3/def2-QZVPPD, in kJ/mol: 6.9 > 6.0 > 5.0).

Aniline···$(CH_4)_2$ complex

The mass selected 2CR2PI spectra of aniline···CH_4 1:1 and 1:2 complexes are presented in Fig. S2 of the supplementary material. The 1:2 complex spectrum is red shifted by 163 cm^{-1} with respect to the aniline monomer origin, a shift approximately twice that of the 1:1 complex (81 cm^{-1}). A similar, nearly additive, shift has previously been observed for benzene and toluene···CH_4 1:2 complexes[77–79] and reflects the two solvent molecules occupying opposite positions with respect to the ring plane. Unlike the related studies of benzene and toluene···CH_4 1:2 complexes, no obvious peak corresponding to the origin of a second isomer (with the two solvent molecules on the same face of the ring) was observed within the proximity of the 1:1 complex origin.

Figure 5 presents an overview of the spectroscopic information collected for the 1:1 and 1:2 complexes, presented with an energy ladder diagram following Fig. 1. The electronic spectra of the complexes, recorded using 2CR2PI, are presented in the lower panels of Fig. 5, while the corresponding ion yield spectra are presented in the upper panels of Fig. 5. The 1:2 complex ion yield curve is similar in shape to that of the 1:1 complex, and an ionization onset was clearly observed around 7.688 eV, lowered as expected relative to the monomer and 1:1 complex.

To determine the experimental S_0 state dissociation energy of the 1:2 complex, 2CAP measurements were employed, as shown in Fig. S3. Here, the mass channel of the $(aniline···CH_4)^+$ fragment was monitored from dissociation of the 1:2 complex by setting the first photon on resonance with the origin of the 1:2 complex and scanning the second above the ionization threshold. As described above for the 1:1 complex, the energetic onset of fragmentation represents the sum of the S_0 state dissociation energy and the adiabatic IP of the 1:1 complex. This method sets an upper limit to the ground state dissociation energy, and using the energy ladder diagram (Fig. 5), we then obtain dissociation energies for the S_1 and D_0 states. These are given with the associated uncertainties in Table II, in units of kJ/mol. We note that VMI experiments for the 1:2 complex were not performed.

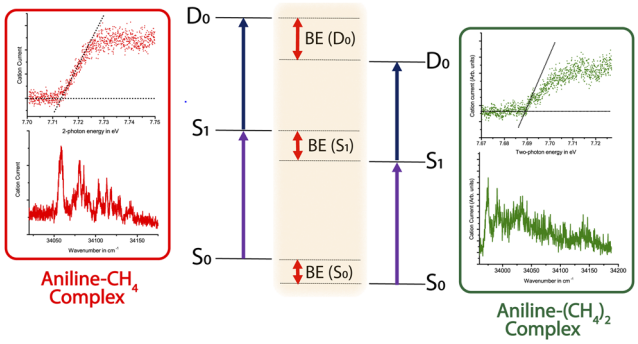

FIG. 5. Spectroscopic data obtained for jet cooled aniline–methane 1:1 and 1:2 complexes, presented with an energy ladder diagram as in Fig. 1. For each species, jet-cooled electronic spectra were obtained using 2CR2PI experiments as described in the text (lower panels). Ion yield spectra, also obtained via 2CR2PI measurements with a tunable second photon, are shown in the upper panels.

In our previous study of the anisole–methane 1:2 complex, we found that the dissociation energy corresponding to a loss of single methane *increased* by 10% with respect to the 1:1 complex across all three states (S_0, S_1, D_0). In contrast, here, we find that the ground state dissociation energy of the 1:2 complex with respect to the loss of one methane is *decreased* by ~10% relative to the 1:1 complex in the S_0 state. This trend is consistent with the inequivalence of the two dissociation sites and, thus, the loss of the more weakly bound methane. The dissociation energy in the S_1 state is decreased by ~10% for the 1:2 complex, while the D_0 (cation radical state) dissociation energy is similar to that found for the 1:1 complex. To gain further insight into these trends, we performed theoretical calculations on the 1:2 complex. Calculations found two minima on the ground state PES, corresponding to structures where

TABLE II. Experimental and calculated dissociation energies for the aniline–methane 1:2 complex.

	Dissociation energy (kJ/mol)		
Method	S_0	S_1	D_0
Experiment (2CAP)	5.7(3)	6.7(3)	7.9(3)
PBE0-D3/def2-QZVPPD	5.9	...	8.3

the two methane molecules are on the same face or opposite faces, respectively, of the aromatic ring. The global minimum energy structure corresponded to the latter, and this is illustrated in Fig. S4 of the supplementary material. Calculations at the (U)PBEO-D3/def2-QZVPPD level well reproduce the observed dissociation energies in the S_0 and D_0 states (see Table II). The coordinates for the optimized structure at this level of theory are provided in Table S3 of the supplementary material.

CONCLUSIONS

To probe cooperativity in C–H/N and C–H/π interactions, we have measured the dissociation energies of aniline···$(CH_4)_n$ (n = 1, 2) van der Waals complexes, in their ground (S_0), excited (S_1), and cation radical (D_0) states, using 2CAP and VMI experiments (the latter for the 1:1 complex only). The dissociation energies of the aniline···CH_4 1:1 complex derived from the 2CAP experiments are consistent with isomeric structure 2, where the methane sits above the aromatic ring but on the same side as the amino hydrogens, and are in good agreement with a range of DFT and *ab initio* methods. We found that the VMI and 2CAP experiments were not in agreement but could be reconciled if it is assumed that dissociation of the complex in the D_0 state leads to the selective population of a low frequency inversion mode in the ionized aniline fragment. This is consistent with the expected (rigid) planarization of the amino group upon ionization. The dual mode of interaction (C/H···π and C/H···N) predicted by the ground state equilibrium geometry of the 1:1 complex is consistent with the large experimental dissociation energy observed when compared to systems exhibiting only C/H···π interactions such as toluene/benzene···CH_4.

Studies of the 1:2 complex show a redshift in the S_0–S_1 spectrum, which is nearly twice that observed for the 1:1 complex, suggestive of a geometry where the two methane moieties lie on opposite faces of the aromatic ring. We find that the ground state dissociation energy of the 1:2 complex with respect to loss of one methane is *decreased* by ~10% relative to the 1:1 complex in the S_0 and D_0 states, consistent with the inequivalency of the two binding sites and loss of the more weakly bound methane. The measured dissociation energies are in good agreement with theoretical expectations.

SUPPLEMENTARY MATERIAL

See the supplementary material for three tables and three figures of additional data. Table S1 shows the calculated data from TDDFT methods for the 1:1 complex, while Tables S2 and S3 show the optimized coordinates for the 1:1 and 1:2 complexes. Figure S1 shows the optimized structure of the cation radical state of the 1:1 complex. Figure S2 compares the 2CR2PI spectra of the aniline monomer and 1:1 and 1:2 aniline–methane complexes. Finally, Fig. S3 shows the optimized structure of the ground state of the 1:2 complex.

DATA AVAILABILITY

The data that support the findings of this study are available within the article and its supplementary material.

REFERENCES

[1]P. Needham, "Hydrogen bonding: Homing in on a tricky chemical concept," Stud. Hist. Philos. Sci. **44**(1), 51–65 (2013).
[2]R. Castellano, "Special Issue: Intramolecular hydrogen bonding," Molecules **19**(10), 15783–15785 (2014).
[3]A. Kovacs and Z. Varga, "Halogen acceptors in hydrogen bonding," Coord. Chem. Rev. **250**(5-6), 710–727 (2006).
[4]D. Kokkin, M. Ivanov, J. Loman, J. Z. Cai, B. Uhler, N. Reilly, R. Rathore, and S. A. Reid, "π-π stacking vs. C–H/π interaction: Excimer formation and charge resonance stabilization in van der Waals clusters of 9, 9′-dimethylfluorene," J. Chem. Phys. **149**(13), 134314 (2018).
[5]M. V. Ivanoy, N. Reilly, B. Uhler, D. Kokkin, R. Rathore, and S. A. Reid, "Cofacially arrayed polyfluorenes: Spontaneous formation of π-stacked assemblies in the gas phase," J. Phys. Chem. Lett. **8**(21), 5272–5276 (2017).
[6]C. Trujillo and G. Sánchez-Sanz, "A study of π-π stacking interactions and aromaticity in polycyclic aromatic hydrocarbon/nucleobase complexes," ChemPhysChem **17**(3), 395–405 (2016).
[7]S. A. Reid, S. Nyambo, L. Muzangwa, and B. Uhler, "π-stacking, C–H/π, and halogen bonding interactions in bromobenzene and mixed bromobenzene-benzene clusters," J. Phys. Chem. A **117**(50), 13556–13563 (2013).
[8]D. Kokkin, M. V. Ivanov, J. Loman, J.-Z. Cai, R. Rathore, and S. A. Reid, "Strength of π-stacking, from neutral to cation: Precision measurement of binding energies in an isolated π-stacked dimer," J. Phys. Chem. Lett. **9**(8), 2058–2061 (2018).
[9]J. T. Makuvaza, D. L. Kokkin, J. L. Loman, and S. A. Reid, "C–H/π and C–H–O interactions in concert: A study of the anisole–methane complex using resonant ionization and velocity mapped ion imaging," J. Phys. Chem. A **123**(13), 2874–2880 (2019).
[10]K. Miyamura, A. Mihara, T. Fujii, Y. Gohshi, and Y. Ishii, "Unusually strong-interactions mediated by both π-π stacking and CH-π interactions present in the dimer of nickel(II) complex coordinated with N-butyl-substituted salen," J. Am. Chem. Soc. **117**(8), 2377–2378 (1995).
[11]L. Muzangwa, S. Nyambo, B. Uhler, and S. A. Reid, "On π-stacking, C–H/π, and halogen bonding interactions in halobenzene clusters: Resonant two-photon ionization studies of chlorobenzene," J. Chem. Phys. **137**(18), 184307 (2012).
[12]S. Jain and K. Vanka, "Can the solvent enhance the rate of chemical reactions through C–H/π interactions? Insights from theory," Phys. Chem. Chem. Phys. **21**(27), 14821–14831 (2019).
[13]M. Brandl, K. Lindauer, M. Meyer, and J. Suhnel, "C–H···O and C–H···N interactions in RNA structures," Theor. Chem. Acc. **101**(1-3), 103–113 (1999).
[14]K. N. Houk, S. Menzer, S. P. Newton, F. M. Raymo, J. F. Stoddart, and D. J. Williams, "[C–H···O] interactions as a control element in supramolecular complexes: Experimental and theoretical evaluation of receptor affinities for the binding of bipyridinium-based guests by catenated hosts," J. Am. Chem. Soc. **121**(7), 1479–1487 (1999).
[15]G. Cavallo, P. Metrangolo, T. Pilati, G. Resnati, M. Sansotera, and G. Terraneo, "Halogen bonding: A general route in anion recognition and coordination," Chem. Soc. Rev. **39**(10), 3772–3783 (2010).
[16]P. Politzer, P. Lane, M. C. Concha, Y. Ma, and J. S. Murray, "An overview of halogen bonding," J. Mol. Model. **13**(2), 305–311 (2007).
[17]S. Sarkhel and G. R. Desiraju, "N–H···O, O–H···O, and C–H···O hydrogen bonds in protein-ligand complexes: Strong and weak interactions in molecular recognition," Proteins: Struct., Funct., Bioinf. **54**(2), 247–259 (2004).
[18]Y. Lu, T. Shi, Y. Wang, H. Yang, X. Yan, X. Luo, H. Jiang, and W. Zhu, "Halogen bonding—A novel interaction for rational drug design?," J. Med. Chem. **52**(9), 2854–2862 (2009).
[19]V. Amendola, L. Fabbrizzi, and L. Mosca, "Anion recognition by hydrogen bonding: Urea-based receptors," Chem. Soc. Rev. **39**(10), 3889–3915 (2010).
[20]M. P. Parker, C. A. Murray, L. R. Hart, B. W. Greenland, W. Hayes, C. J. Cardin, and H. M. Colquhoun, "Mutual complexation between π–π stacked molecular tweezers," Cryst. Growth Des. **18**(1), 386–392 (2018).
[21]P. Metrangolo, F. Meyer, T. Pilati, G. Resnati, and G. Terraneo, "Halogen bonding in supramolecular chemistry," Angew. Chem., Int. Ed. **47**(33), 6114–6127 (2008).

[22]D. H. Levy, C. A. Haynam, and D. V. Brumbaugh, "Spectroscopy and photophysics of organic clusters," Faraday Discuss. Chem. Soc. **73**, 137–151 (1982).
[23]C. Y. Ng, "Molecular-beam photoionization studies of molecules and clusters," Adv. Chem. Phys. **52**, 263–362 (2007).
[24]F. G. Celii and K. C. Janda, "Vibrational spectroscopy, photochemistry, and photophysics of molecular clusters," Chem. Rev. **86**(3), 507–520 (1986).
[25]J. R. Cable, M. J. Tubergen, and D. H. Levy, "The electronic-spectra of small peptides in the gas-phase," Faraday Discuss. Chem. Soc. **86**, 143–152 (1988).
[26]U. Buck, "Structure, energetics, dynamics. Structure and dynamics of size selected molecular clusters," Ber. Bunsen. Phys. Chem. **96**(9), 1275–1284 (1992).
[27]R. N. Pribble, C. Gruenloh, and T. S. Zwier, "The ultraviolet and infrared spectroscopy of (benzene)$_2$-(CH$_3$OH)$_3$ isomeric clusters," Chem. Phys. Lett. **262**(5), 627–632 (1996).
[28]C. J. Gruenloh, J. R. Carney, F. C. Hagemeister, C. A. Arrington, T. S. Zwier, S. Y. Fredericks, J. T. Wood, and K. D. Jordan, "Resonant ion-dip infrared spectroscopy of the S_4 and D_{2d} wafer octamers in benzene-(water)$_8$ and benzene$_2$-(water)$_8$," J. Chem. Phys. **109**(16), 6601–6614 (1998).
[29]F. C. Hagemeister, C. J. Gruenloh, and T. S. Zwier, "Resonant ion-dip infrared spectroscopy of benzene-(water)$_n$–(methanol)$_m$ clusters with n + m = 4, 5," Chem. Phys. **239**(1-3), 83–96 (1998).
[30]C. J. Gruenloh, F. C. Hagemeister, J. R. Carney, and T. S. Zwier, "Resonant ion-dip infrared spectroscopy of ternary benzene–(water)$_n$(methanol)$_m$ hydrogen-bonded clusters," J. Phys. Chem. A **103**(4), 503–513 (1999).
[31]G. M. Florio, C. J. Gruenloh, R. C. Quimpo, and T. S. Zwier, "The infrared spectroscopy of hydrogen-bonded bridges: 2-pyridone-(water)$_n$ and 2-hydroxypyridine-(water)$_n$ clusters, n = 1, 2," J. Chem. Phys. **113**(24), 11143–11153 (2000).
[32]D. R. Borst, J. R. Roscioli, D. W. Pratt, G. M. Florio, T. S. Zwier, A. Muller, and S. Leutwyler, "Hydrogen bonding and tunneling in the 2-pyridone·2-hydroxypyridine dimer. Effect of electronic excitation," Chem. Phys. **283**(1-2), 341–354 (2002).
[33]D. J. Moll, G. R. Parker, and A. Kuppermann, "Time-resolved two-color photoacoustic and multiphoton ionization spectroscopy of aniline," J. Chem. Phys. **80**(10), 4808–4816 (1984).
[34]M. A. Smith, J. W. Hager, and S. C. Wallace, "Two color photoionization spectroscopy of jet cooled aniline: Vibrational frequencies of the aniline approximately-$\tilde{X}^2B_1$ radical cation," J. Chem. Phys. **80**(7), 3097–3105 (1984).
[35]J. Lemaire, I. Dimicoli, F. Piuzzi, and R. Botter, "Two-color photoionization spectroscopy of polyatomic-molecules and cations: Aniline, phenol and phenetole," Chem. Phys. **115**(1), 119–128 (1987).
[36]J. A. Syage and J. E. Wessel, "Ion dip spectroscopy of higher excited vibronic states of aniline," J. Chem. Phys. **85**(11), 6806–6807 (1986).
[37]K. Yamanouchi, S. Isogai, S. Tsuchiya, and K. Kuchitsu, "Laser-induced fluorescence spectroscopy of He-, Ne-, Ar-, and Kr-aniline van der Waals complexes in a supersonic free jet. Analysis of rotational contours," Chem. Phys. **116**(1), 123–132 (1987).
[38]M. Becucci, G. Pietraperzia, E. Castellucci, and P. Brechignac, "Dynamics of vibronically excited states of the aniline–neon van der Waals complex: Vibrational predissociation versus intramolecular vibrational redistribution," Chem. Phys. Lett. **390**(1-3), 29–34 (2004).
[39]M. Becucci, G. Pietraperzia, N. M. Lakin, E. Castellucci, and P. Brechignac, "High-resolution spectroscopy of aniline-rare gas van der Waals complexes: Results and comparison with theoretical predictions," Chem. Phys. Lett. **260**(1-2), 87–94 (1996).
[40]R. G. Satink, J. M. Bakker, G. Meijer, and G. von Helden, "Vibrational lifetimes of aniline–noble gas complexes," Chem. Phys. Lett. **359**(1-2), 163–168 (2002).
[41]E. J. Bieske, M. W. Rainbird, and A. E. W. Knight, "The van der Waals vibrations of aniline-(argon)$_2$ in the S_1 electronic state," J. Chem. Phys. **94**(11), 7019–7028 (1991).
[42]E. J. Bieske, A. S. Uichanco, M. W. Rainbird, and A. E. W. Knight, "Mass selected resonance enhanced multiphoton ionization spectroscopy of aniline–Ar$_n$ (n = 3, 4, 5, . . .) van der Waals complexes," J. Chem. Phys. **94**(11), 7029–7037 (1991).
[43]B. Coutant and P. Brechignac, "Anomalous complex shift of low-frequency out-of-plane vibrations in aniline-M van der Waals complexes (M = He, Ne, Ar)," J. Chem. Phys. **100**(10), 7087–7092 (1994).
[44]S. Douin, P. Hermine, P. Parneix, and P. Brechignac, "Site specificity of solvent shifts as revealed by ionization threshold in aniline–(argon)$_n$ clusters," J. Chem. Phys. **97**(3), 2160–2162 (1992).
[45]P. Parneix and P. Bréchignac, "The hindering of the inversion motion in the van der Waals aniline-Ar$_n$ clusters: An adiabatic molecular dynamics simulation for n = 1–3," J. Chem. Phys. **108**(5), 1932–1939 (1998).
[46]P. Parneix, P. Bréchignac, and F. G. Amar, "Isomer specific evaporation rates: The case of aniline-Ar$_2$," J. Chem. Phys. **104**(3), 983–991 (1996).
[47]P. Parneix, N. Halberstadt, P. Bréchignac, F. G. Amar, A. van der Avoird, and J. W. I. van Bladel, "Quantum calculation of vibrational states in the aniline-argon van der Waals cluster," J. Chem. Phys. **98**(4), 2709–2719 (1993).
[48]H. Piest, G. von Helden, and G. Meijer, "Infrared spectroscopy of jet-cooled neutral and ionized aniline-Ar," J. Chem. Phys. **110**(4), 2010–2015 (1999).
[49]J. Makarewicz, "Structure and dynamics of the aniline-argon complex as derived from its potential energy surface," J. Phys. Chem. A **111**(8), 1498–1507 (2007).
[50]T. Pino, P. Parneix, S. Douin, and P. Bréchignac, "Solvation dynamics of large van der Waals aniline-Ar$_n$ clusters: Experiment and theory," J. Phys. Chem. A **108**(36), 7364–7371 (2004).
[51]S. Douin, P. Parneix, and P. Brechignac, "Solvent shift of the ionization-potential of the aniline-argon system," Z. Phys. D: At., Mol. Clusters **21**(4), 343–348 (1991).
[52]T. Nakanaga, K. Sugawara, K. Kawamata, and F. Ito, "Infrared depletion spectroscopy of aniline-NH_3 and aniline-NH_3^+ clusters in a supersonic jet," Chem. Phys. Lett. **267**(5-6), 491–495 (1997).
[53]J. A. Fernandez and E. R. Bernstein, "Structure, binding energy, and intermolecular modes for the aniline/ammonia van der Waals clusters," J. Chem. Phys. **106**(8), 3029–3037 (1997).
[54]M. Foltin, G. J. Stueber, and E. R. Bernstein, "Dynamics of neutral cluster growth and cluster ion fragmentation for toluene/water, aniline/argon, and 4-fluorostyrene/argon clusters: Covariance mapping of the mass spectral data," J. Chem. Phys. **109**(11), 4342–4360 (1998).
[55]I. León, P. F. Arnáiz, I. Usabiaga, and J. A. Fernández, "Mass resolved IR spectroscopy of aniline-water aggregates," Phys. Chem. Chem. Phys. **18**(39), 27336–27341 (2016).
[56]E. R. Bernstein, K. Law, and M. Schauer, "Molecular supersonic jet studies of aniline solvation by helium and methane," J. Chem. Phys. **80**(2), 634–644 (1984).
[57]M. R. Nimlos, M. A. Young, E. R. Bernstein, and D. F. Kelley, "Vibrational dynamics of aniline(Ar)$_1$ and aniline(CH$_4$)$_1$ clusters," J. Chem. Phys. **91**(9), 5268–5277 (1989).
[58]X. Zhang, J. M. Smith, and J. L. Knee, "High resolution threshold photoelectron spectroscopy of aniline and aniline van der Waals complexes," J. Chem. Phys. **97**(5), 2843–2860 (1992).
[59]J. M. Smith, X. Zhang, and J. L. Knee, "Aniline-CH$_4$ S_1 vibrational dynamics studied with picosecond photoelectron spectroscopy," J. Chem. Phys. **99**(4), 2550–2559 (1993).
[60]P. K. Chowdhury, K. Sugawara, T. Nakanaga, and H. Takeo, "Structure of the aniline–benzene and aniline–cyclohexane clusters based on infrared depletion spectroscopy," Chem. Phys. Lett. **285**(1-2), 77–82 (1998).
[61]K. Ohashi, Y. Inokuchi, H. Izutsu, K. Hino, N. Yamamoto, N. Nishi, and H. Sekiya, "Electronic and vibrational spectra of aniline–benzene hetero-dimer and aniline homo-dimer ions," Chem. Phys. Lett. **323**(1-2), 43–48 (2000).
[62]K. Ohashi, Y. Inokuchi, N. Nishi, and H. Sekiya, "Intermolecular interactions in aniline–benzene hetero-trimer and aniline homo-trimer ions," Chem. Phys. Lett. **357**(3-4), 223–229 (2002).
[63]P. K. Chowdhury, "Infrared depletion spectroscopy of the hydrogen-bonded aniline–diethylamine (C_6H_5–NH_2···NHC_4H_{10}) complex produced in supersonic jet," J. Phys. Chem. A **107**(30), 5692–5696 (2003).
[64]K. Kawamata, P. K. Chowdhury, F. Ito, K.-i. Sugawara, and T. Nakanaga, "Investigation of the N–H stretching vibrations of the aniline–pyrrole binary complex and its cation by infrared depletion spectroscopy," J. Phys. Chem. A **102**(25), 4788–4793 (1998).
[65]T. Nakanaga and F. Ito, "Investigations on the hydrogen bond interaction in the aniline–furan complex and its cation by infrared depletion spectroscopy," J. Phys. Chem. A **103**(28), 5440–5445 (1999).

[66]N. Yamamoto, K. Hino, K. Mogi, K. Ohashi, Y. Sakai, and H. Sekiya, "Hole-burning spectroscopy and *ab initio* calculations for the aniline dimer," Chem. Phys. Lett. **342**(3-4), 417–424 (2001).
[67]D. Schemmel and M. Schutz, "Molecular aniline clusters. II. The low-lying electronic excited states," J. Chem. Phys. **133**(13), 134307 (2010).
[68]D. Schemmel and M. Schutz, "Molecular aniline clusters. I. The electronic ground state," J. Chem. Phys. **132**(17), 174303 (2010).
[69]K.-i. Sugawara, J. Miyawaki, T. Nakanaga, H. Takeo, G. Lembach, S. Djafari, H.-D. Barth, and B. Brutschy, "Infrared depletion spectroscopy of the aniline dimer," J. Phys. Chem. **100**(43), 17145–17147 (1996).
[70]R. Montero, I. Lamas, I. León, J. A. Fernández, and A. Longarte, "Excited state dynamics of aniline homoclusters," Phys. Chem. Chem. Phys. **21**(6), 3098–3105 (2019).
[71]V. R. Thalladi, A. Gehrke, and R. Boese, "C–H group acidity and the nature of C–H···N interactions: Crystal structural analysis of pyrazine and methyl substituted pyrazines," New J. Chem. **24**(6), 463–470 (2000).
[72]N.-B. Wong, Y.-S. Cheung, D. Y. Wu, Y. Ren, X. Wang, A. M. Tian, and W.-K. Li, "A theoretical study of the C–H···N hydrogen bond in the methane–ammonia complex," J. Mol. Struct.: THEOCHEM **507**, 153–156 (2000).
[73]C. E. Marjo, R. Bishop, D. C. Craig, and M. L. Scudder, "Crystal engineering involving C–H···N weak hydrogen bonds: A diquinoxaline lattice inclusion host with a preference for polychlorocarbon guests," Eur. J. Org. Chem. **2001**(5), 863–873.
[74]C. S. Lai, F. Mohr, and E. R. T. Tiekink, "The importance of C–H···N, C–H···π and π···π interactions in the crystal packing of the isomeric N^1,N^4-bis((pyridine-*n*-yl)methylene)-cyclohexane-1,4-diamines, n = 2, 3 and 4," CrystEngComm **8**(12), 909–915 (2006).
[75]S. F. Alshahateet, R. Bishop, D. C. Craig, and M. L. Scudder, "Dimeric C–H···N interactions and the crystal engineering of new inclusion host molecules," CrystEngComm **48**, 225 (2001).
[76]E. Bosch, "Role of sp-C–H···N hydrogen bonding in crystal engineering," Cryst. Growth Des. **10**(8), 3808–3813 (2010).
[77]M. Schauer and E. R. Bernstein, "Molecular jet study of the solvation of benzene by methane, ethane, and propane," J. Chem. Phys. **82**(2), 726–735 (1985).
[78]M. Schauer, K. Law, and E. R. Bernstein, "Supersonic molecular jet studies of toluene–helium and toluene-methane clusters," J. Chem. Phys. **81**(1), 49–56 (1984).
[79]M. Schauer, K. S. Law, and E. R. Bernstein, "Molecular jet study of the solvation of toluene by methane, ethane, and propane," J. Chem. Phys. **82**(2), 736–746 (1985).
[80]J. A. Menapace and E. R. Bernstein, "van der Waals modes of solute solvent clusters: Benzene-methane, benzene-deuteriomethane, and benzene-carbon tetrafluoride," J. Phys. Chem. **91**(11), 2843–2848 (1987).
[81]S. Karthikeyan, V. Ramanathan, and B. K. Mishra, "Influence of the substituents on the CH···π interaction: Benzene-methane complex," J. Phys. Chem. A **117**(30), 6687–6694 (2013).
[82]J. Li and R.-Q. Zhang, "Strong orbital deformation due to CH–π interaction in the benzene–methane complex," Phys. Chem. Chem. Phys. **17**(44), 29489–29491 (2015).
[83]W. E. Hatton, D. L. Hildenbrand, G. C. Sinke, and D. R. Stull, "Chemical thermodynamic properties of aniline," J. Chem. Eng. Data **7**, 229–231 (1962).
[84]F. Kraus, E. Gregorek, and H. Weyssenh, "Absolute fluorescence lifetimes and quantum yields of substituted anilines in gas-phase," Z. Phys. Chem. **82**(1-4), 139–146 (1972).
[85]H. V. Weyssenhoff and F. Kraus, "Vibronic structure in fluorescence lifetimes and quantum yields of aniline vapor," J. Chem. Phys. **54**(6), 2387 (1971).
[86]H. Krieg and S. Grimme, "Thermochemical benchmarking of hydrocarbon bond separation reaction energies: Jacob's ladder is not reversed!," Mol. Phys. **108**(19-20), 2655–2666 (2010).
[87]X. Song, M. Yang, E. R. Davidson, and J. P. Reilly, "Zero kinetic-energy photoelectron-spectra of jet-cooled aniline," J. Chem. Phys. **99**(5), 3224–3233 (1993).
[88]F. Mazzoni, M. Pasquini, G. Pietraperzia, and M. Becucci, "Binding energy determination in a π-stacked aromatic cluster: The anisole dimer," Phys. Chem. Chem. Phys. **15**(27), 11268–11274 (2013).